Mater. Res. Soc. Symp. Proc. Vol. 1395 © 2012 Materials Research Society
DOI: 10.1557/opl.2012.340

# Comparative electrode kinetics of micro and nano-crystalline boron doped diamond.

E. Saito, A.F. Azevedo, F.A. Souza, N.G. Ferreira, M.R. Baldan
Instituto Nacional de Pesquisas Espaciais (INPE) -12201-970
São José dos Campos, Brasil

## ABSTRACT

Comparative study of boron doped micro/nanocrystalline diamond (BDD/BDND) electrodes was performed using electrochemical impedance spectroscopy measurements (EIS). The morphological and structural characterizations of BDD/BDND films were analyzed by scanning electron microscopy and Raman scattering spectroscopy. The films were grown with different boron amounts added in the feed gas. The boron source for BDND was smaller in concentration than that for BDD sample. Nonetheless, differential capacitance (Mott-Schottky plots) and heterogeneous charge transfer constant results showed similar doping level for both electrodes. This behavior indicated the high efficiency to dope nanocrystalline diamond films.

## INTRODUCTION

Boron doped micro/nanocrystalline diamond (BDD/BDND) films have been extensively studied due to their singular properties mainly for electrochemical applications[1].Particularly, BDD films are produced in the doping range from semiconductor to semi-metallic behavior ($10^{17}$ – $10^{22}$ $cm^{-3}$ boron atoms). For low carrier concentration, boron atoms most probably replace the carbon sites substitutionally with an impurity level with activation energy of 0.37 eV [2]. As the boron concentration is increased, the wave functions of holes bound to an impurity site can overlap and the impurity level evolves into an impurity "band". This is an approach of a metallic state in the vicinity of the semiconductor-metal transition. About undoped nanocrystalline diamond films, the conductivity mechanism can be compared to amorphous semiconductor, with bandgap reduced by band approximation and several states at the bandgap by $sp^2$ bonding[3,4].

Although the doping mechanism is described as similar for BDD or BDND films, the conductivity process for both electrodes is not completely understood. The electrode activity is strongly influenced by surface termination[5,6,7] and grain boundaries and $sp^2$ presence at this region[8]. Therefore, this work is devoted to evaluate comparatively the kinetic performance of BDD/BDND for electrochemical applications. In this way, the electrochemical impedance spectroscopy (EIS) appeared as an important technique. It permits to obtain the heterogeneous charge transfer constant ($k^0$), from the charge transfer resistance, by fitting the equivalent electric circuit model. The heterogeneous rate constant obtained by EIS technique is more precise than that obtained by other potential sweep techniques. The films were grown with different boron amounts added in the feed gas. The boron source for BDND was 15 times smaller in

concentration than that for BDD sample. To reduce the influence of high hydrogenated surface the samples were exposed to atmospheric air until stabilization of surface (constant contact angle – not shown). Besides, the morphological, the structural, and the electrochemical results are discussed considering the efficiency to dope BDD/BDND films.

## EXPERIMENTAL DETAILS

Both BDD/BDND films were grown on p-type silicon (100) substrate by hot filament chemical vapor deposition (HFCVD). The substrates were submitted to seeding pre-treatment [9]. The BDD film was grown for 10 h at 50 Torr and 800 °C with 1.0 % $CH_4$ and 99 % $H_2$ while the BDND was grown for 10 h at 30 Torr and 650 °C with 38,3% of $H_2$, 1,0% of $CH_4$ e 60,7% of Ar. Boron was obtained from $H_2$ forced to pass through a bubbler containing $B_2O_3$ dissolved in methanol. The doping was varied from B/C rations of 2,000 and 30,000 ppm for BDND and BDD, respectively. The samples morphologies were evaluated by Scanning Electron Microscopy (SEM – Jeol - Model JSM-15310). The Micro-Raman spectra were recorded by Renishaw system 2000 in backscattering configuration at room temperature, employing 514 nm Argon-ion laser. The electrochemical impedance spectroscopy (EIS) and differential capacitance measurements were performed with Autolab PGSTAT-302 with potentiostatic control in a three electrode cell with a platinum mesh as a counter and Ag/AgCl as reference electrode. The sample geometric areas were 0.12$cm^2$. The EIS measurements were made at the frequency range of $2.0x10^4$ Hz to$10^{-2}$ Hz with the redox pair ($10^{-3}ML^{-1}$ Ferro/Ferricyanide in a KCl $1ML^{-1}$). The differential capacitance measurements were taken in 0.5 Mol $L^{-1}$ solution at $1.0 \times 10^3$ Hz. All measurements were conducted at room temperature

## DISCUSSION

### Morphological and Physical analysis

The SEM images for BDD/BDND films are shown in figure 1(a). The images confirmed the polycrystalline films that uniformly coated the substrates. BDD film demonstrated faceted grains with symmetrical and smooth faces with uniform texture and predominant (111) orientation. For BDND film (figure1 (a) inset) the surface is flat and with morphology quite similar to unfaceted CVD diamond called "ballas-like". The grains tended to form small agglomerates with around 0,5 μm of diameter, suggesting a secondary nucleation or re-nucleation process. The average roughness Rq was evaluated from AFM images around 350 and 25 nm, for BDND and BDD, respectively (not shown). The Raman spectra of both films are shown in figure 1 (b) with the effect of boron doping in the spectral features. For BDD film, the Raman peak at around 1332 $cm^{-1}$ is clearly observed corresponding to the vibration of a diamond first-order phonon[10]. In addition, there is the appearance of the broad bands at ~ 500 and ~1220 $cm^{-1}$. The broad peak at 500 $cm^{-1}$ refers to the boron pair's vibration while the band at ~1220 $cm^{-1}$ concerning the diamond lattice distortion induced by the boron incorporation. Eight features were identified in the Raman spectrum of BDND film. The diamond peak is visible and

shifted to lower wavenumber (1300 $cm^{-1}$) that is related to impurities formed in heavily doped films showing a metallic like conductivity[11]. The bands at 1350 and 1550 $cm^{-1}$ are related to the D and G band, respectively. Besides, the spectrum exhibited a shoulder at 1150 $cm^{-1}$ and a peak at 1490 $cm^{-1}$ related to transpolyacetylene (TPA) at the grain boundaries of BDND surface. The broad bands at around 500 and 1220 $cm^{-1}$ present in these films are still subject to an intense debate. They have been associated with the actual boron incorporation in the lattice, rather than the hole concentration [1]. The presence of the 500 $cm^{-1}$ peak is attributed to the concentration increase of the boron pairs. The Raman spectra and quality of both samples is supported by several works [12,13]

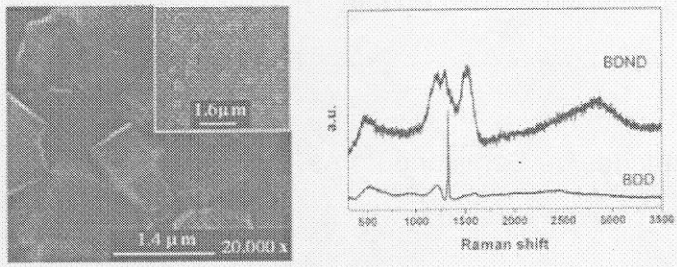


Figure 1. (a) –Scanning electron microscopy images of the films BDD and BDND (figure inset). (b) The Raman spectra of both samples.

## Electrochemical characterization

Mott-Schottky plots (MSP) measurements for BDD/BDND samples are presented in figure 2 (a). The MSP measurement and posterior calculations were made considering the series RC equivalent circuit as the interface. The graphs were interpreted formally basing on the sigh of the line slopes as MSP drawn for semiconductor electrodes. From the linear segment of the curves the flat-band potentials $V_{fb}$ were estimated at 1.05 and 0.89 V x Ag/AgCl while from the curve slopes the donor concentrations were evaluated as $N_D = 0{,}9 \times 10^{20}$ $cm^{-3}$ and $N_D = 1.0 \times 10^{20}$ $cm^{-3}$ for BDD and BDND, respectively. These values are very close considering the doping characteristics of both electrodes.

The electrochemical performance of the films was evaluated by electrochemical impedance spectroscopy (EIS) measurements at open circuit potential. The EIS is a well established theory that describes the response of a circuit to an alternating current or voltage as a function of applied frequency. Therefore, EIS is an efficient method to probe and model the interfacial characterization of the diamond electrodes. The amplitude selection was made as predicted by Orazem to avoid non linear effects[14]. After all measurements, the Kramers Kronig transforms (KK) was conducted by software guided by Boukamp's work [15]. Figures 2(b) shows the response obtained from EIS for the BDD and the BDND films. The data were

fitted using the adapted Randles-Ershler equivalent circuit (Figure 2(b) inset) with passive elements described as following: R1 as the solution resistance, R2 as the heterogeneous charge transfer resistance, Q1 as the constant phase element (CPE) associated with the double layer capacitance and Q2 is associated to the Warburg element (diffusion controlled). The Q1 was used as proposed by Hsu and Mansfield to fit the double layer[16]. The deviations from ideal capacitor response of double layer are attributed to roughness, heterogeneities, distribution of relaxation time constants, pores, etc [17]. The table 1 presents the data obtained from the equivalent circuit of the EIS measurement carried out for BDD and BDND samples.

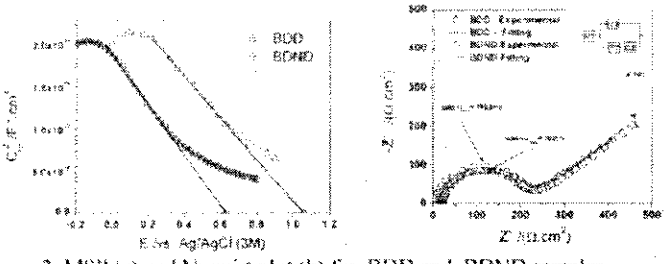


Figure 2. MSP (a) and Nyquist plot (b) for BDD and BDND samples.

As showed by the Nyquist plots, similar responsiveness was obtained for both electrodes in the EIS measurements using the redox couple ($10^{-3}$mol $L^{-1}$ Ferro/Ferricyanide in a KCl 1mol $L^{-1}$). At high and intermediate frequency values a characteristic semicircle attributed to parallel RC is observed. The elements R2 and Q1 are relative to charge transfer resistance and double layer capacitance (fitted using the CPE), respectively. The diffusion controlled response is confirmed at lower frequencies and fitted by Q2. The whole parameters obtained by Complex Non Linear Least Squares (CNLS) fitting are presented in table 1.

Table 1 – Parameters obtained from the fitting of the equivalent circuit.

| Element | BDD | BDND | Units |
|---|---|---|---|
| R1 | 4.94±0.19 | 23.25±0.39 | $\Omega.cm^2$ |
| Q1 | (5.94±0.44)x$10^{-6}$ | (4.53±0.31)x$10^{-6}$ | $\Omega^{-1}.cm^{-2}s^{\alpha}$ |
| $\alpha_1$ | 0.91±0.08 | 0.89±0.09 | - |
| R2 | 262.62±3.51 | 238.14±3.91 | $\Omega$ |
| Q2 | (3.92±0.07)x$10^{-2}$ | (3.08±0.05) x$10^{-2}$ | $\Omega^{-1}.cm^{-2}s^{\alpha}$ |
| $\alpha_2$ | 0.49±0.05 | 0.44±0.83 | - |

The electrode performance can be characterized quantitatively by using a known electron redox couple and calculating the kinetic rate constant. $k^0$ was evaluated for both electrodes from the equation (1) using the electrode geometric area[18].

$$k^{o} = \frac{RT}{n^2 F^2 R_{ct}[\ ]} \qquad (1)$$

where R is the universal gas constant (8,31 J $K^{-1}$mol$L^{-1}$), T is the temperature(K), F is the faraday constant (9,64 x $10^4$ s A $mol^{-1}$), n is the number of electrons involved in reaction ,and [ ] is the concentration of the redox species (mol $L^{-1}$). The values obtained from equation (1) are presented in Table 2. The double layer capacitance of both films was estimated for BDD and BDND as 5,94 μF $cm^{-2}$ and 4,53 μF.$cm^{-2}$, respectively. The deviation from ideal capacitor is adjusted by the constant phase element Q1. The heterogeneous charge transfer rate constant calculated is inferior to the state-of the art micro and nanocrystalline films [19,20] but

Table 2 - Heterogeneous charge transfer obtained from Eq. 1.

| Sample | Charge transfer constant ($K^{o}$) |
|---|---|
| BDD | $0.49 \times 10^{-03}$ |
| BDND | $0.54 \times 10^{-03}$ |

The electrochemical measurements from EIS showed similar heterogeneous rate constant values for both electrodes, independently of the doping level used to produce them. This result is a strong indicative that the efficiency to dope BDND is higher than that for BDD electrode. We can speculate about this difference considering some morphological and physical aspects of both electrodes. As measured by Williams et al. using High Resolution Electron Energy Loss Spectroscopy (HREELS) technique, for undoped diamond films, the $sp^2$ presence at the grain boundaries presents high concentration of hydrogen[21]. In the case of the BDND, the renucleation process is enhanced firstly by the addition of an inert gas (Ar) and simultaneously by the boron insertion that leads to high $sp^2$ content of such film. Therefore, the high conductivity of BDND may be attributed to two contributions due to its high $sp^2$ content. The first one related to the high hydrogen concentration and the second associated to the $\pi$ and $\pi^*$ states around Fermi level assured by the $sp^2$ presence [21].

## CONCLUSIONS

The morphological and structural characterization conducted by SEM and Raman analysis confirmed the quality of BDD and BDND films for electrochemical applications. The differential capacitance showed similar slopes, indicating a high efficiency to dope ultananocrystalline films. The electrochemical characterization, conducted by EIS, also showed comparable values of heterogeneous rate transfer constants for BDD and BDND. The electrochemical performance of BDND may also be attributed to the $\pi$ and $\pi^*$ states at its grains boundaries that enhanced the conductivity of this electrode. This study showed the possibility to control the film growth parameters to achieve similar electrochemical responsiveness by controlling the film grain size concomitantly to its boron content. And besides the low charge transfer rate constant, similar values were obtained with great differences in dopant solution concentration(15 times).

## ACKNOWLEDGMENTS

The authors would like to thanks M.L.Brison for SEM images. The authors are very grateful to Brazilian research agencies Fapesp, Capes and CNPq for the financial support.

## REFERENCES

1.Y. Einaga. Journal of Applied Electrochemistry. Volume 40. Number 10. 1807-1816.
2.T.Yokoya;T.Nakamura;T.Matsushita;T.Muro;E.Ikenaga;M.Kobata;K.Kobayashi; Y.Takano;M.Nagao;T. Takenouchi; H.Kawarada; T.Oguchi. T.New Diamond and Frontier Carbon Technology.Vol. 17, No. 1 2007.
3. M. Nesladek, K.Meykens, L.M. Stals,M. Vanecek, J. Rosa, *Phys. Review B.* 54 (8) (1996) 5552–5561.
4. P. Achatz, O.A. Williams, P. Bruno, D.M. Gruen, J.A. Garrido, M. Stutzmann, Phys. Review B 74 (2006).
5. N. Simon, H. Girard, D. Ballutaud, S. Ghodbane, A. Deneuville, M. Herlem, A. Etcheberry. Diam. Relat. Mater., 14 (2005), 1179-1182.
6.
7.J. van de Lagemaat, D. Vanmaekelbergh, J.J. Kelly. J. Electroanal. Chem., 475 (1999), pp. 139–151.
8. P.W. May,W.J. Ludlowa,M. Hannawaya, P.J. Heardb, J.A. Smitha, K.N. Rosser. Diam. and Relat. Materials. 17, 2, 2008, 105–117.
9. B.V. Spitsyn, L.L. Bouilov, B.V. Derjaguin, Journal of Crystal Growth 52 (APR) (1981) 219–226.
10. D.S. Knight and W.B. White, J. Mater. Reser. 4 (1989) 385-393.
11. M. Bernard, C. Baron and A. Deneuville, Diam. Relat. Mater., vol.13, n°.4-8, pp.896-899, 2004.
12. P.W.May, W.J. Ludlow, M.Hannaway, J.A. Smith, K.N.Rosser,and P.J.Heard. MRS Proceedings 2007 1039 : 1039-P17-03.
13. P.W. May, W.J. Ludlow, M. Hannaway, P.J. Heard, J.A. Smith, K.N. Rosser. Diamond and Related Materials. 17,2,2008,105–117.
14. B. Hirschorn; B.Tribollet; M. E. Orazem – Isr. Journ. Chemistry ,48,133-142(2008).
15. B. A. Boukamp – Solid. State Ionics -18-19,136-140, (1986).
16. C.S. Hsu, F. Mansfeld, Corrosion, 57(2001) 747.
17. B.Emmanuel ,Journal of Electroanalytical Chemistry 624 (2008) 14–20.
18. A.J. Bard, L.R. Faulkner, Electrochemical Methods, Wiley, New York, 1980.
19. M.C. Granger,M. Witek,J.Xu,J.Wang,M.Hupert,A. Hanks,M. D. Koppang,J.E. Butler,G. Lucazeau,M.Mermoux,J. W. Strojek, and Greg M. Swain .Anal. Chem., 2000, 72 (16), 3793–3804.
20. M. Hupert,A. Muck,J. Wang,J. Stotter,Z. Cvackova,S. Haymond,Y. Show,G.M. Swain. Diam. and Relat. Materials.V.12, 10–11, 2003, Pages 1940–1949.
21.O.A. Williams, M. Nesladek, M. Daenen, S. Michaelson, A. Hoffman, E. Osawa, K.Haenen,R.B.Jackman. DiamondandRelatedMaterials17(7–10) (2008) 1080–1088.